THE JOURNAL OF PHYSICAL CHEMISTRY C LETTERS

2008, *112,* 13346–13348
Published on Web 08/13/2008

Electrochemical Identification of Metallic and Semiconducting Single-Walled Carbon Nanotubes

Peng Qian,[†] Zhongyun Wu,*[,†] Peng Diao,[‡] Guoming Zhang,[†] Jin Zhang,[†] and Zhongfan Liu*[,†]

Centre for Nanoscale Science and Technology (CNST), State Key Laboratory for Structural Chemistry of Unstable and Stable Species, Beijing National Laboratory for Molecular Sciences, College of Chemistry and Molecular Engineering, Peking University, Beijing 100871, P. R. China, and Department of Applied Chemistry, School of Materials Science and Engineering, Beijing University of Aeronautics and Astronautics, Beijing 100083, P. R. China

Received: July 9, 2008; Revised Manuscript Received: August 2, 2008

Single-walled carbon nanotubes (SWNTs) are promising building blocks for nanoelectronics. However, because of the mixture of metallic and semiconducting single-walled carbon nanotubes (m-SWNTs and s-SWNTs), it is necessary to identify them for nanodevice integerations. In this work, we have observed obvious electrodeposition differences of ultralong m-SWNTs and s-SWNTs. Using high-resolution atomic force microscopy (AFM) and field emission scanning electron microscopy (FE-SEM), particle densities along different carbon nanotubes were examined. Interestingly, m-SWNTs and s-SWNTs showed obviously different deposition behaviors, i.e., exponential decay of particle densities with different decay coefficients. This electrochemical approach can be used for a simple identification of m-SWNTs and s-SWNTs.

Single-walled carbon nanotubes (SWNTs) can be either metallic or semiconducting depending on their chiralities and diameters.[1] As-grown SWNTs are a mixture of metallic and semiconducting single-walled carbon nanotubes (m-SWNTs and s-SWNTs) that hinder their applications in nanoelectronics,[2] chemical,[3] and biological nanosensors.[4,5] Several techniques have been established to identify m- and s-SWNTs. Resonance Raman spectroscopy is often used to determine the metallic and semiconducting characteristics of carbon nanotubes. But only the SWNTs satisfying the enhanced resonance rules can be detected with specific laser energy.[6] On the other hand, the electrical measurements[7] can clearly tell the transport characteristics of m- and s-SWNTs. However, the electrical measurements require the SWNT is properly fixed on two electrodes with good ohmic contact by a lithography process that is expensive and time-consuming. Herein we report electrochemical identification of m- and s-SWNTs by simple electrodeposition[8−11] using metal nanoparticles as labels (Figure 1).

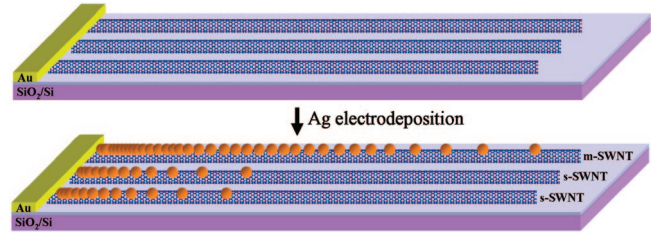

Figure 1. Schematic illustration of electrochemical identification of m-SWNTs and s-SWNTs.

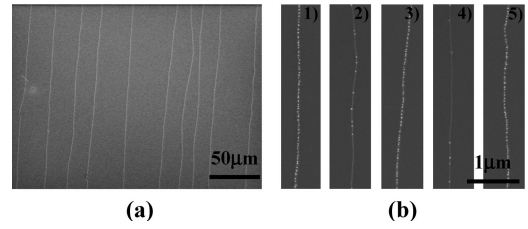

Figure 2. (a) Typical SEM image of ultralong SWNTs array. (b) SEM images of Ag-decorated SWNTs with obviously different particle distribution after electrodeposition at −0.6 V for 80 ms. They are put together for easy comparison. (1), (3), and (5) are m-SWNTs. (2) and (4) are s-SWNTs.

Ultralong, well-separated, and aligned SWNTs were grown by catalytic chemical vapor deposition (CVD) of ethanol[12] on marked silicon wafers with 800 nm thermal oxide layer on the surface. SEM (HITACHI S-4800) was used to characterize the as-grown SWNTs, and typical results are shown in Figure 2a. Prior to SWNTs growth,[13] several groups of Pt microelectrodes were patterned on the substrates by magnetron sputtering. These Pt electrodes were used to identify m- and s-SWNTs by standard electrical measurements. Only the SWNTs that have contact with Pt electrodes were taken as samples. The transport characteristics of each sampled SWNT were carried out using a low-current measurement system (Keithley 4200) coupled with a four-probe station (TMC). Tapping mode AFM (Veeco Nanoscope III SPM) was used to determine the diameter of each sampled SWNT to confirm that they are single-walled. Before electrodeposition, a gold electrode with titanium as an adhesive layer was thermally evaporated on the starting end of SWNTs to make good electrical contact with SWNTs, as shown schematically in Figure 1. The average length of SWNT working electrodes was about 3−5 mm. The electrodeposition of Ag

* To whom correspondence should be addressed. E-mail: zfliu@pku.edu.cn.
[†] Peking University.
[‡] Beijing University of Aeronautics and Astronautics.

10.1021/jp806043j CCC: $40.75

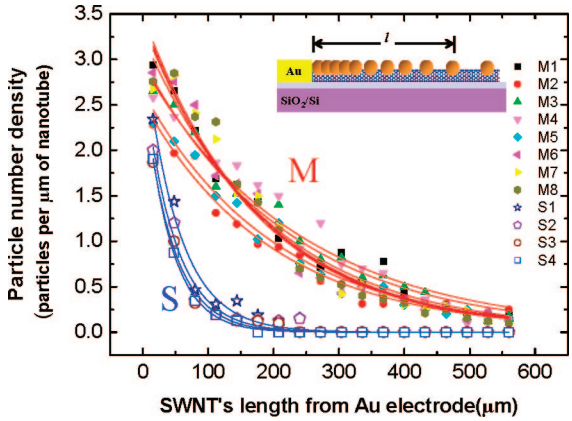

Figure 3. Particle number density of 12 Ag-decorated SWNTs with −0.6 V for 40 ms. They are denoted as M1−M8 for m-SWNTs (solid marks) and S1−S4 for s-SWNTs (hollow marks). Solid curves are exponential decay fits of these data points.

nanoparticles was carried out on an electrochemical workstation (CHI 660B) at constant potential in a homemade three-electrode cell. The electrolyte solution contained 1 mM $AgNO_3$ and 0.2 M KNO_3 (see Supporting Information for all experimental details).

Figure 2b shows three typical SEM images of m-SWNTs and two images of s-SWNTs after silver electrodeposition. All of the five SEM images, which were taken at the same distance of about 90 μm from Au electrode on the same substrate, were put together for easy comparison. From Figure 2b, it is easy to find that m- and s-SWNTs demonstrate remarkably different deposition behaviors. Three m-SWNTs (denoted as 1, 3, and 5) show nearly continuous nanoparticles distribution, while two s-SWNTs (denoted as 2 and 4) show a much smaller number of scattered silver nanoparticles at the same distance from the common gold electrode. Typical tapping mode AFM images of an m-SWNT and an s-SWNT after Ag decoration show the same deposition difference (see Supporting Information). To clearly demonstrate the different deposition behaviors of m- and s-SWNTs, the variation of the particle density (particles per micrometer of SWNT) as a function of carbon nanotubes length was obtained by counting the particle number along each SWNT in the SEM images. Twelve SWNTs whose transport properties were determined by electrical measurements were examined, including eight m-SWNTs and four s-SWNTs. The results are shown in Figure 3.

Although the particle densities along all SWNTs exponentially decrease with the increase of tube length, the s-SWNTs exhibit a remarkably faster decay rate compared to that of m-SWNTs. Solid curves in Figure 3 are exponential decay fits of original data points for clearly showing the distribution difference of m- and s-SWNTs. The form of exponential decay used is $D = D_0 \exp(-\tau l)$. D is the particle density at a certain length of SWNT, while D_0 is the particle density at the starting end (zero SWNT length). l is the length of SWNT from the common Au electrode, and τ is the decay coefficient, which implies the decay rate of particle density. All fitted D_0 and τ data are shown in Table 1. The mean values of τ are 0.0051 ± 0.0004 and 0.022 ± 0.002 μm^{-1} for m- and s-SWNTs, respectively, indicating the great difference of electrodeposition behavior between m- and s-SWNTs.

We believe that the different tube-length-dependent potential drop of m- and s-SWNTs dominates the experimental results. In conventional electrochemical experiments using a metal macroelectrode, the electrode is usually considered as having

TABLE 1: Statistical Information of 12 SWNTs

no.	d^a (nm)	ω^b (cm^{-1})	ON/OFF ratio^c	D_0 (particles/μm)	τ (μm^{-1})	M/S
1	1.7		2.4	3.27	0.00517	*M*
2	1.8		4.6	2.54	0.00510	*M*
3	2.0		4.3	2.99	0.00454	*M*
4	2.2		3.0	2.93	0.00457	*M*
5	1.8		6.3	2.65	0.00492	*M*
6	2.1		3.8	3.44	0.00564	*M*
7	1.7		10.2	3.39	0.00545	*M*
8	1.9		8.6	3.49	0.00561	*M*
9	1.6	151.0	2.7×10^4	3.22	0.0192	*S*
10	1.8	139.3	3.2×10^4	2.88	0.0215	*S*
11	2.0		7.3×10^3	2.71	0.0227	*S*
12	2.1	123.0	4.6×10^4	2.85	0.0248	*S*

[a] The diameters of SWNTs obtained by AFM. [b] Raman shift of SWNTs. [c] Determined by electrical measurements.

the same potential due to its very small resistivity. As for a carbon nanotube, the resistivity can not be ignored because of its one-dimension (1D) structure. The resistivity of an SWNT is usually described by the electron mean free path L_e. The larger the L_e value, the smaller the resistivity. Usually, m-SWNTs have a much longer electron mean free path than s-SWNTs because the former have a much stronger suppression for the electron scattering.[14] The 1D resistivity of s-SWNTs is considered about 10 times larger than that of m-SWNTs,[15,16] resulting in a much larger potential drop along s-SWNTs. On the other hand, it has been demonstrated that the solution acts as a gate for s-SWNTs and has a great effect on their electrochemical behaviors. When negative potentials is applied to an s-SWNT, i.e., electrodeposition of Ag in our work, s-SWNT is in the "much resistive" state (the Fermi level of s-SWNT is present in the band gap), while an m-SWNT is almost not affected by the solution gate.[9,17]

The mean value of D_0 is 3.08 ± 0.37 particles/μm for m-SWNTs and 2.92 ± 0.22 particles/μm for s-SWNTs, implying that when the length of SWNT is decreased to several micrometers, the electrodeposition difference of m- and s-SWNTs become much less observable. This is in good agreement with previous experimental and theoretical works in which the short m- and s-SWNTs yield similar steady-state voltammetric behaviors.[17,18] It is obvious that when SWNTs are very short, the difference of the potential drop along the m- and s-SWNTs is not enough to make an observable variation of the particle density. The particle density along SWNTs reflects the rate of electrochemical-induced nucleation of silver on different section of SWNTs. The position-dependent electronucleation rate along SWNTs, which can be described by Butler−Volmer equation,[19] is determined by the actually applied potential at each nucleation site. We are currently trying to make a model to explore the reason of this electrodeposition difference.

In summary, we have demonstrated an electrochemical approach for identifying metallic and semiconducting single-walled carbon nanotubes. m- and s-SWNTs showed different elcctrodeposition behaviors, i.e., exponential decay dependence of particle density on the length of carbon nanotubes. Potential drop along nanotubes and electrochemical gating may play a dominant role in recent experiment results. The aligned ultralong SWNTs prepared on solid substrates have found wide applications in studying the fundamentals of nanoelectronics and in developing SWNT-based electronic devices. The ability for the differentiation between metallic and semiconducting SWNTs is essential for SWNT-based nanoelectronics. This work provides a simple and effective strategy to determine the electronic properties of a number of parallel ultralong SWNTs in one

measurement, showing great potentials in the studies of SWNT-based nanoelectronics. We expect this electrochemical method can be used as a simple, effective, and reliable approach for identifying metallic and semiconducting SWNTs accompanied with other conventional methods.

Acknowledgment. The research was supported by National Natural Science Foundation of China (grants nos. 90606022, 90406024) and MOST (2006CB932701, 2006CB932403, 2007CB936203).

Supporting Information Available: Experimental details, results of electrical measurements, Raman spectra of m- and s-SWNTs, SEM, and AFM images of Ag-decorated m- and s-SWNTs. This material is available free of charge via the Internet at http://pubs.acs.org.

References and Notes

(1) Avouris, P. *Acc. Chem. Res.* **2002**, *35*, 1026.
(2) Zhang, G.; Qi, P.; Wang, X.; Lu, Y.; Li, X.; Tu, R.; Bangsaruntip, S.; Mann, D.; Zhang, L.; Dai, H. *Science* **2006**, *314*, 974.
(3) Kong, J.; Franklin, N. R.; Zhou, C.; Chapline, M. G.; Peng, S.; Cho, K.; Dai, H. *Science* **2000**, *287*, 622.
(4) Besteman, K.; L, J.-O.; Wiertz, F. G. M.; Heering, H. A.; Dekker, C. *Nano Lett.* **2003**, *3*, 727.
(5) Eugenii Katz, I. W. *ChemPhysChem* **2004**, *5*, 1084.
(6) Dresselhaus, M. S.; Dresselhaus, G.; Jorio, A.; Souza Filho, A. G.; Pimenta, M. A.; Saito, R. *Acc. Chem. Res.* **2002**, *35*, 1070.
(7) Tans, S. J.; Verschueren, A. R. M.; Dekker, C. *Nature* **1998**, *393*, 49.
(8) Day, T. M.; Unwin, P. R.; Wilson, N. R.; Macpherson, J. V. *J. Am. Chem. Soc.* **2005**, *127*, 10639.
(9) Day, T. M.; Wilson, N. R.; Macpherson, J. V. *J. Am. Chem. Soc.* **2004**, *126*, 16724.
(10) Quinn, B. M.; Dekker, C.; Lemay, S. G. *J. Am. Chem. Soc.* **2005**, *127*, 6146.
(11) Day, T. M.; Unwin, P. R.; Macpherson, J. V. *Nano Lett.* **2007**, *7*, 51.
(12) Yao, Y.; Li, Q.; Zhang, J.; Liu, R.; Jiao, L.; Zhu, Y. T.; Liu, Z. *Nat. Mater.* **2007**, *6*, 283.
(13) Wilson, N. R.; Guille, M.; Dumitrescu, I.; Fernandez, V. R.; Rudd, N. C.; Williams, C. G.; Unwin, P. R.; Macpherson, J. V. *Anal. Chem.* **2006**, *78*, 7006.
(14) Purewal, M. S.; Hong, B. H.; Ravi, A.; Chandra, B.; Hone, J.; Kim, P. *Phys. Rev. Lett.* **2007**, *98*, 186808.
(15) Park, J.-Y.; Rosenblatt, S.; Yaish, Y.; Sazonova, V.; Ustunel, H.; Braig, S.; Arias, T. A.; Brouwer, P. W.; McEuen, P. L. *Nano Lett.* **2004**, *4*, 517.
(16) Javey, A.; Guo, J.; Wang, Q.; Lundstrom, M.; Dai, H. *Nature* **2003**, *424*, 654.
(17) Heller, I.; Kong, J.; Williams, K. A.; Dekker, C.; Lemay, S. G. *J. Am. Chem. Soc.* **2006**, *128*, 7353.
(18) Heller, I.; Kong, J.; Heering, H. A.; Williams, K. A.; Lemay, S. G.; Dekker, C. *Nano Lett.* **2005**, *5*, 137.
(19) Bard, A. J.; Faulkner, L. R. *Electrochemical Methods: Fundamental and Applications*, 2nd ed.; J. Wiley & Sons: New York, 2000.

JP806043J